LOAN DOCUMENT

PHOTOGRAPH THIS SHEET

DTIC ACCESSION NUMBER

LEVEL

INVENTORY

WL-TR-96-2093

DOCUMENT IDENTIFICATION

DISTRIBUTION STATEMENT A
Approved for public release;
Distribution Unlimited

DISTRIBUTION STATEMENT

ACCESSION FOR
NTIS GRA&I ☒
DTIC TRAC ☐
UNANNOUNCED ☐
JUSTIFICATION

BY

DISTRIBUTION/

AVAILABILITY CODES

DISTRIBUTION	AVAILABILITY AND/OR SPECIAL	
A-1		

DISTRIBUTION STAMP

DATE ACCESSIONED

DTIC QUALITY INSPECTED 1

DATE RETURNED

A-1 19960812 156

DATE RECEIVED IN DTIC

REGISTERED OR CERTIFIED NUMBER

PHOTOGRAPH THIS SHEET AND RETURN TO DTIC-FDAC

DTIC FORM 70A JUN 90

DOCUMENT PROCESSING SHEET

PREVIOUS EDITIONS MAY BE USED UNTIL STOCK IS EXHAUSTED.

LOAN DOCUMENT

HANDLE WITH CARE

DISCLAIMER NOTICE

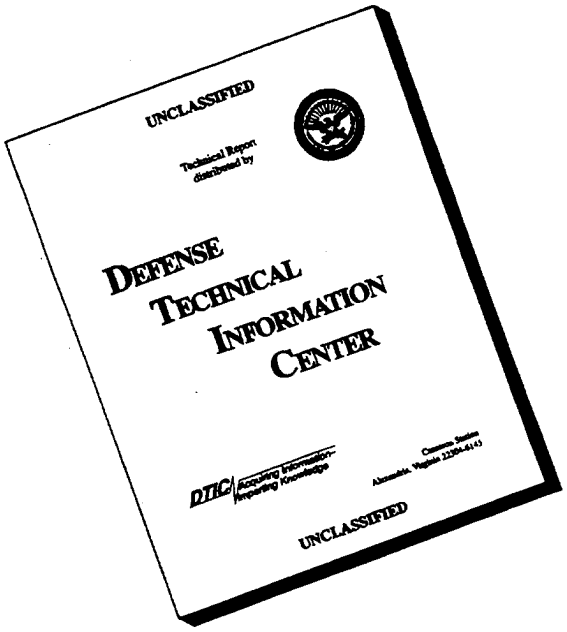

THIS DOCUMENT IS BEST QUALITY AVAILABLE. THE COPY FURNISHED TO DTIC CONTAINED A SIGNIFICANT NUMBER OF PAGES WHICH DO NOT REPRODUCE LEGIBLY.

WL-TR-96-2093

AN EXPERIMENTAL INVESTIGATION OF HEAT TRANSFER, TRANSITION AND SEPARATION ON TURBINE BLADES AT LOW REYNOLDS NUMBER AND HIGH TURBULENCE INTENSITY

James W. Baughn
Robert J. Butler
Aaron R. Byerley
Richard B. Rivir

1995

FINAL REPORT 1 NOVEMBER 1995--9 JULY 1996

Approved for public release; distribution unlimited

AERO PROPULSION & POWER DIRECTORATE
WRIGHT LABORATORY
AIR FORCE MATERIEL COMMAND
WRIGHT-PATTERSON AIR FORCE BASE, OH 45433-7650

NOTICE

WHEN GOVERNMENT DRAWINGS, SPECIFICATIONS, OR OTHER DATA ARE USED FOR ANY PURPOSE OTHER THAN IN CONNECTION WITH A DEFINITELY GOVERNMENT-RELATED PROCUREMENT, THE UNITED STATES GOVERNMENT INCURS NO RESPONSIBILITY OR ANY OBLIGATION WHATSOEVER. THE FACT THAT THE GOVERNMENT MAY HAVE FORMULATED OR IN ANY WAY SUPPLIED THE SAID DRAWINGS, SPECIFICATIONS, OR OTHER DATA, IS NOT TO BE REGARDED BY IMPLICATION, OR OTHERWISE IN any MANNER CONSTRUED, AS LICENSING THE HOLDER, OR ANY OTHER PERSON OR CORPORATION; OR AS CONVEYING ANY RIGHTS OR PERMISSION TO MANUFACTURE, USE, OR SELL ANY PATENTED INVENTION THAT MAY IN ANY WAY BE RELATED THERETO.

THIS REPORT IS RELEASABLE TO THE NATIONAL TECHNICAL INFORMATION SERVICE (NTIS). AT NTIS, IT WILL BE AVAILABLE TO THE GENERAL PUBLIC, INCLUDING FOREIGN NATIONS.

THE TECHNICAL REPORT HAS BEEN REVIEWED AND IS APPROVED FOR PUBLICATION.

RICHARD B. RIVIR
Manager, Aerothermal Research
Turbine Branch
Turbine Engine Division
Aero Propulsion & Power Directorate

CHARLES D. MACARTHUR
Chief
Turbine Branch
Turbine Engine Division
Aero Propulsion & Power Directorate

RICHARD J. HILL
Chief of Technology
Turbine Engine Division
Aero Propulsion & Power Directorate

IF YOUR ADDRESS HAS CHANGED, IF YOU WISH TO BE REMOVED FROM OUR MAILING LIST, OR IF THE ADDRESSEE IS NO LONGER EMPLOYED BY YOUR ORGANIZATION PLEASE NOTIFY WL/POTT, WPAFB OH 45433-7650 TO HELP MAINTAIN A CURRENT MAILING LIST.

REPORT DOCUMENTATION PAGE

Form Approved
OMB No. 0704-0188

1. AGENCY USE ONLY *(Leave blank)*	2. REPORT DATE	3. REPORT TYPE AND DATES COVERED
	1995	Final 1 Nov 95 - 9 Jul 96

4. TITLE AND SUBTITLE

An Experimental Investigation of Heat Transfer, Transition and Separation on Turbine Blades at Low Reynolds Number and High Turbulence Intensity

5. FUNDING NUMBERS

PE 61102F
JON 2307S315

6. AUTHOR(S)

James W. Baughn, Robert J. Butler, Aaron R. Byerley, Richard B. Rivir

7. PERFORMING ORGANIZATION NAME(S) AND ADDRESS(ES)

Aero Propulsion & Power Directorate
Wright Laboratory
Air Force Materiel Command
Wright-Patterson Air Force Base, OH 45433-7650

8. PERFORMING ORGANIZATION REPORT NUMBER

9. SPONSORING / MONITORING AGENCY NAME(S) AND ADDRESS(ES)

Aero Propulsion & Power Directorate
Wright Laboratory
Air Force Materiel Command
Wright-Patterson Air Force Base, OH 45433-7650
POC: Richard B Rivir, WL/POTT, 513-255-5132

10. SPONSORING / MONITORING AGENCY REPORT NUMBER

WL-TR-96-2093

11. SUPPLEMENTARY NOTES

12a. DISTRIBUTION / AVAILABILITY STATEMENT

APPROVED FOR PUBLIC RELEASE; DISTRIBUTION IS UNLIMITED

12b. DISTRIBUTION CODE

13. ABSTRACT *(Maximum 200 words)*

The effects of turbulence intensity on the heat transfer distribution, transition and flow separation on a turbine blade was investigated at low Reynolds numbers. Measurements were performed in linear cascades (at both UCDavis and the USAF Academy) at low Reynolds number (67,000 to 144,000) representative of low pressure turbine stages at high altitude. Nominal turbulence intensities of 1% and 10% (generated with biplane lattice grids) were used. The heat transfer was measured with the uniform heat flux (UHF) or heated-coating method. The heated-coating was a gold-film and liquid crystals were used for the surface temperature measurement. A novel laser-tuft surface flow visualization method was also used. For low turbulence levels (1%) the pressure side of the blade exhibited streaks of varying heat transfer possibly associated with Taylor-Gortler vortices. With grid turbulence (10%) these streaks disappeared on the pressure side and the heat transfer nearly doubled. Gird turbulence also increased the heat transfer on the leading edge and suction surface, while advancing the location of boundary layer transition. Good agreement was generally found between the UCDavis and USAFA data. These cascade results compare favorably to those that have been reported with rotation.

14. SUBJECT TERMS			15. NUMBER OF PAGES 19
			16. PRICE CODE
17. SECURITY CLASSIFICATION OF REPORT	18. SECURITY CLASSIFICATION OF THIS PAGE	19. SECURITY CLASSIFICATION OF ABSTRACT	20. LIMITATION OF ABSTRACT
UNCLASSIFIED	UNCLASSIFIED	UNCLASSIFIED	SAR

GENERAL INSTRUCTIONS FOR COMPLETING SF 298

The Report Documentation Page (RDP) is used in announcing and cataloging reports. It is important that this information be consistent with the rest of the report, particularly the cover and title page. Instructions for filling in each block of the form follow. It is important to ***stay within the lines*** to meet ***optical scanning requirements***.

Block 1. Agency Use Only *(Leave blank)*.

Block 2. Report Date. Full publication date including day, month, and year, if available (e.g. 1 Jan 88). Must cite at least the year.

Block 3. Type of Report and Dates Covered. State whether report is interim, final, etc. If applicable, enter inclusive report dates (e.g. 10 Jun 87 - 30 Jun 88).

Block 4. Title and Subtitle. A title is taken from the part of the report that provides the most meaningful and complete information. When a report is prepared in more than one volume, repeat the primary title, add volume number, and include subtitle for the specific volume. On classified documents enter the title classification in parentheses.

Block 5. Funding Numbers. To include contract and grant numbers; may include program element number(s), project number(s), task number(s), and work unit number(s). Use the following labels:

C	- Contract	**PR**	- Project
G	- Grant	**TA**	- Task
PE	- Program Element	**WU**	- Work Unit Accession No.

Block 6. Author(s). Name(s) of person(s) responsible for writing the report, performing the research, or credited with the content of the report. If editor or compiler, this should follow the name(s).

Block 7. Performing Organization Name(s) and Address(es). Self-explanatory.

Block 8. Performing Organization Report Number. Enter the unique alphanumeric report number(s) assigned by the organization performing the report.

Block 9. Sponsoring/Monitoring Agency Name(s) and Address(es). Self-explanatory.

Block 10. Sponsoring/Monitoring Agency Report Number. *(If known)*

Block 11. Supplementary Notes. Enter information not included elsewhere such as: Prepared in cooperation with...; Trans. of...; To be published in.... When a report is revised, include a statement whether the new report supersedes or supplements the older report.

Block 12a. Distribution/Availability Statement. Denotes public availability or limitations. Cite any availability to the public. Enter additional limitations or special markings in all capitals (e.g. NOFORN, REL, ITAR).

- **DOD** - See DoDD 5230.24, "Distribution Statements on Technical Documents."
- **DOE** - See authorities.
- **NASA** - See Handbook NHB 2200.2.
- **NTIS** - Leave blank.

Block 12b. Distribution Code.

- **DOD** - Leave blank.
- **DOE** - Enter DOE distribution categories from the Standard Distribution for Unclassified Scientific and Technical Reports.
- **NASA** - Leave blank.
- **NTIS** - Leave blank.

Block 13. Abstract. Include a brief *(Maximum 200 words)* factual summary of the most significant information contained in the report.

Block 14. Subject Terms. Keywords or phrases identifying major subjects in the report.

Block 15. Number of Pages. Enter the total number of pages.

Block 16. Price Code. Enter appropriate price code *(NTIS only)*.

Blocks 17. - 19. Security Classifications. Self-explanatory. Enter U.S. Security Classification in accordance with U.S. Security Regulations (i.e., UNCLASSIFIED). If form contains classified information, stamp classification on the top and bottom of the page.

Block 20. Limitation of Abstract. This block must be completed to assign a limitation to the abstract. Enter either UL (unlimited) or SAR (same as report). An entry in this block is necessary if the abstract is to be limited. If blank, the abstract is assumed to be unlimited.

To be published in bound proceedings of the 1995 International Mechanical Engineering Congress and Exposition. Session Chairman has recommended further publication in the ASME Journal of Turbomachinery.

AN EXPERIMENTAL INVESTIGATION OF HEAT TRANSFER, TRANSITION AND SEPARATION ON TURBINE BLADES AT LOW REYNOLDS NUMBER AND HIGH TURBULENCE INTENSITY

James W. Baughn*
Mechanical and Aeronautical Engineering
University of California
Davis, California

Robert J. Butler
Department of Aeronautics
USAF Academy
Colorado Springs, Colorado

Aaron R. Byerley
Department of Mechanical Engineering
Mercer University
Macon, Georgia

Richard B. Rivir
Aero Propulsion and Power Directorate
Wright Laboratory
Wright-Patterson AFB, Ohio

ABSTRACT

The effects of turbulence intensity on the heat transfer distribution, transition and flow separation on a turbine blade was investigated at low Reynolds numbers. Measurements were performed in linear cascades (at both UCDavis and the USAF Academy) at low Reynolds number (67,000 to 144,000) representative of low pressure turbine stages at high altitude. Nominal turbulence intensities of 1% and 10% (generated with biplane lattice grids) were used. The heat transfer was measured with the uniform heat flux (UHF) or heated-coating method. The heated-coating was a gold-film and liquid crystals were used for the surface temperature measurement. A novel laser-tuft surface flow visualization method was also used. For low turbulence levels (1%) the pressure side of the blade exhibited streaks of varying heat transfer possibly associated with Taylor-Görtler vortices. With grid turbulence (10%) these streaks disappeared on the pressure side and the heat transfer nearly doubled. Grid turbulence also increased the heat transfer on the leading edge and suction surface, while advancing the location of boundary layer transition. Good agreement was generally found between the UCDavis and USAFA data. These cascade results compare favorably to those that have been reported with rotation.

* Authors are listed in alphabetical order

NOMENCLATURE

B_x	airfoil axial chord
B_1	air inlet angle
B_2	air exit angle
h	local heat transfer coefficient
i	electric current
l	length of gold sheet
p	pitch distance between turbine blades
q''	local surface heating (electrical) per unit area
q_c''	convective heat transfer flux
q_L''	conductive heat transfer loss
Re	Reynolds number based on inlet conditions and axial chord
R_{40}	resistance of gold at 40° C
R_{40}''	resistance per square of gold at 40° C
s	surface arc length
St	Stanton number based on inlet conditions
T_{LC}	temperature when liquid crystal is yellow
T_∞	free-stream air temperature
Tu	turbulence intensity
w	width of gold film
x	distance measured in axial chord direction
y	distance measured perpendicular to axial chord
β	cascade flow angle measured relative to the y-axis
δx	experimental uncertainty in the parameter x
ε	surface emissivity
σ	Stefan-Boltzman constant

BACKGROUND

Since the development of the gas turbine engine, improvements in engine efficiency have been gained through improvements to individual engine components. Much of this attention has been on understanding and improving turbine blade cooling and materials. An actual turbine rotor blade is three dimensional and rotates in an extreme environment (high temperature and turbulence). Due to practical limitations, little fundamental research on turbine blades is performed in operating gas turbine engines. Instead, different types of experimental approaches are used to simplify studies of the flow and heat transfer in turbine stages. In general, we can divide these different approaches into two categories, cascade (linear and annular) and rotating facilities. The cascade and rotating facilities can be further subdivided depending on whether they use steady-state or transient testing techniques. For completeness a brief review of turbine testing is included here. For additional background and information on computational techniques, the thorough review by Simoneau and Simon (1993) should be consulted.

Cascade testing is generally the simplest model of the gas turbine flow path. Gostelow (1984) defines a cascade to be "an infinite row of equidistant similar bodies". "The cascade plane is obtained by viewing along the blade axis... a cut is made along the streamline and then viewed in a direction parallel to the blade axis or stacking line". A linear cascade is formed if this "cut" is unrolled to form a two-dimensional row of blades. An annular cascade is axis-symmetric and "consists of a row of blades mounted between two co-axial surfaces of revolution". Testing similarity is improved, with a corresponding increase in difficulty, when rotation is added. Both cascade and rotating facilities can operate under steady-state or transient running conditions. For the brief review here we group tests into the following four types: steady-state cascade, transient cascade, steady-state rotating, and transient rotating.

Steady-state linear cascade research started with very early work by Wilson and Pope (1954). The United Technologies Research Center (UTRC) group ran important test cases using a now common blade shape in a linear cascade [Langston et al. (1977) and Graziani (1980)], later they used this same shape in rotating tests. This blade shape is commonly referred to as the Langston blade or Langston geometry. Detailed aerodynamic measurements were performed on the Langston geometry at Virginia Polytechnic Institute [Moore and Ransmayr (1984a, 1984b), Moore and Adhye (1985), Moore and Moore (1985), and Moore et al. (1987)]. Heat transfer data was collected on the Langston geometry at NASA Lewis [Hippensteele et al. (1985), Boyle and Russell (1990)] and numerical computations were performed by Boyle (1991). Priddy and Bayley (1988) investigated the effect of turbulence on turbine blade heat transfer. Turbulence and wake effects were also studied in the linear cascade test facility at the Institute of Thermal Turbomachinery (ITS), Karlsruhe, Germany by Dullenkopf et al. (1991), and Dullenkopf and Mayle (1994). At Detroit Diesel Allison, Nealy et al. (1984) and York et al. (1984) investigated the heat transfer on nozzle guide vanes.

Transient cascade experiments have been performed at Oxford's isentropic light piston tunnel. This facility has been used for transient heat transfer tests on a linear cascade by Schultz et al. (1980) and wake effects by Ashworth et al. (1985). An annular cascade section was added to the Oxford tunnel and transient heat transfer tests were performed on nozzle guide vanes by Wedlake et al. (1989), and Harasgama and Wedlake (1991).

Steady-state rotating experiments were also performed by the UTRC group in addition to their linear cascade work. They performed many investigations using a steady-state rotating facility with Langston's mean blade geometry [Dring et al. (1986), Blair et al. (1989a), Blair et al. (1989b), and Blair (1994)]. At MIT, a rotating blowdown tunnel which operates under both transient and steady-state conditions was used to measure turbine blade heat transfer which was compared to Oxford's cascade data (Guenette et al., 1989). A new rotating facility is being run at Pennsylvania State University and is discussed in Lakshminarayana et al. (1992).

Transient rotating experiments were done by Dunn and Stoddard (1979) who began an impressive amount of research carried out in a shock tube driven transient rotating facility developed at Calspan. Heat transfer tests were performed on the Garrett TFE 731-2 [Dunn and Stoddard (1979), Dunn and Hause (1982), Dunn et al. (1984a, 1984b), and Dunn (1990)], Teledyne CAE 702 HP [Dunn and Chupp (1988), and Dunn et al. (1989)], and the Rocketdyne Space Shuttle (Dunn et al., 1994) engines in this facility. Oxford is also performing transient rotational tests. Their heat transfer technique and instrumentation is explained by Ainsworth et al. (1989).

The type of facility and its operating condition (transient versus steady-state) is important when considering the method for measuring heat transfer. Most transient facilities use a method developed by Schultz and Jones (1973). These methods use a resistance gage to measure the transient surface temperature and a circuit (which is an electrical equivalent to the semi-infinite conduction equation) to determine the surface heat flux. This method

or one based on the same idea was used in all of the following tests: Schultz et al. (1980), Ashworth et al. (1985), Ainsworth et al. (1989), Wedlake et al. (1989), Harasgama and Wedlake (1991), Dunn and Stoddard (1979), Dunn and Hause (1982), Dunn et al. (1984a, 1984b), and Dunn (1990), Dunn and Chupp (1988), and Dunn et al. (1989), and Dunn et al. (1994). These techniques have the ability to give high frequency heat transfer fluctuations. Guenette et al. (1989) developed a similar transient method but it used two temperature sensitive resistance gages with an insulating material between them. Like the other methods, this gage uses the outer temperature for high frequency data, but this uses a temperature difference across a known insulating resistance to measure the low frequency heat transfer.

Steady-state cascade and rotating facilities use other methods to measure heat transfer. Wilson and Pope (1954) used individually heated Nichrome strips to create a uniform temperature, the local heat transfer could then be determined on each strip. Turner (1971) developed a technique which used cooling tubes running through a turbine blade model. The surface temperatures and the advected energy across each tube were measured. These measurements were then used as boundary conditions solving Laplace's equation for conduction inside the blade, the local heat transfer was determined by the local conduction surface temperature gradient. Similar methods were later used by Nealy et al. (1984), York et al. (1984), Dullenkopf et al. (1991), and Dullenkopf and Mayle (1994). Probably the most popular method used in steady-state tests is called the uniform heat flux (UHF) or heated-coating method.

The uniform heat flux (UHF) or heated-coating method has a very long history. The general idea is to measure the local surface temperatures on a model which is producing a uniform heat transfer flux (typically electrical resistance heating) from a heated-coating on the test surface. The local heat transfer coefficient can be calculated by knowing the power into the surface, local surface temperature, heated area, and free-stream temperature. Variations on the uniform heat flux technique involve different ways to measure the surface temperature and different ways to produce the heat flux.

A general overview of the many researchers who have used UHF methods is included. Early work using this technique used thermocouples in order to measure the local surface temperature. Local heat transfer coefficients were measured for a cylinder in cross-flow by Giedt (1949) who used thermocouples and nichrome ribbon to produce the electrical resistance heat flux. Wilson and Pope (1954) used a similar technique to measure the heat transfer on turbine blade shapes in very early cascade tunnel testing. Simonich and Bradshaw (1978) used steel shim strips to produce the needed heat flux to measure the effect of free-stream turbulence on turbulent boundary layers. O'Brien et al. (1986) used inconel foil and thermocouples on one of three different cylinder models to compare different heat transfer techniques. Some other more recent techniques have used liquid crystals on the test surface to measure surface temperature. Cooper et al. (1975) used carbon impregnated paper to produce the heat flux and liquid crystals to test a cylinder in cross-flow. A similar technique was used by Hippensteele et al. (1985) to measure the local heat transfer around a turbine blade in a cascade tunnel. Like the present method, Baughn et al. (1989) used a thin polyester surface with vacuum deposited gold and liquid crystals to compare uniform heat flux and transient tests on a pin fin. Endwall heat transfer in a cascade tunnel was investigated by Boyle and Russell (1990) using a thin metallic foil and liquid crystals. Graziani (1980), Dring et al. (1986), Blair et al. (1989a), Blair et al. (1989b), and Blair (1994) used this technique with thermocouples to measure surface temperature. Like the present method, Hippensteele et al. (1985), and Boyle and Russell (1990) used liquid crystals to measure surface temperature.

In all UHF method designs, the test surface has to be covered with some type of heater element in order to produce the uniform heat flux. This usually limits the application of this technique to flat surfaces or surfaces with curvature in only one direction.

The present research uses gold-film for the heater similar to that of Baughn et al. (1989) and liquid crystals to measure the heat transfer on a turbine blade in linear cascade facilities at UCDavis and the USAF Academy.

LINEAR CASCADE TEST FACILITIES

Two linear cascade facilities were used in the present research. One is at the USAF Academy and is a closed loop wind tunnel specifically designed for use as a linear cascade facility. The other is at UCDavis and was developed by adding a turning cascade section onto an existing UCDavis wind tunnel. In this case the wind tunnel is open loop and is driven by a 50 HP constant speed motor operating a centrifugal compressor. Stilling chamber with screens are used upstream of the wind tunnel nozzles to reduce free-stream turbulence.

The geometry of the linear cascade sections and of the turbine blades are shown in Figures 1 and 2 respectively. The parameters for the UCDavis and USAFA tunnels are in Table I. The x-axis is defined in the axial direction. Cascade angles are defined relative to the y-axis.

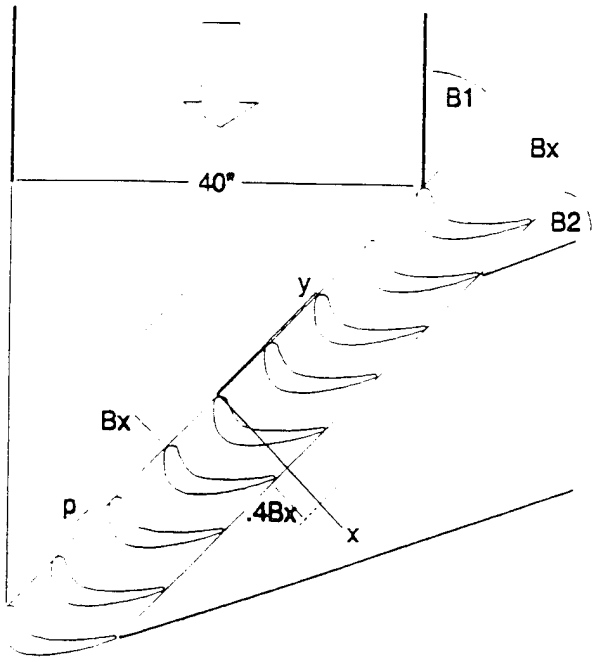

FIGURE 1. CASCADE GEOMETRY

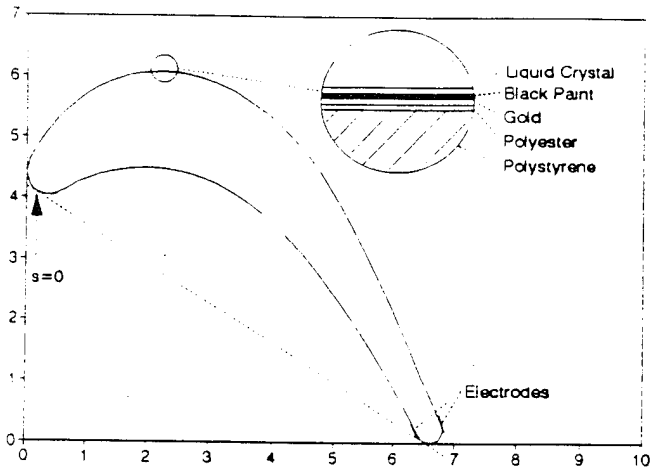

FIGURE 2. BLADE GEOMETRY WITH SURFACE CROSS-SECTION

TABLE I. CASCADE TUNNEL COMPARISON

	UCDavis	USAF Academy
Operation	Open Loop	Closed Loop
Axial Chord (Bx)	0.171 m	0.166 m
Blade Pitch (p)	159 m	196 m
Pitch/Axial Chord	.93	1.18
Span/Axial Chord	3.56	3.97
Inlet Camber Angle	44°	46.5°
Exit Camber Angle	26°	23.5°
Air Inlet Angle (B_1)	44.7°	49°
Air Exit Angle (B_2)	26°	23.5°
Grid	Perpendicular to free-stream	Parallel to cascade
Turbulence (clean,grid)	1% 10%	.5% 9%
Re (clean,grid)	144,000 134,000	110,000 110,000

For the UCDavis cascade section, the cascade angles are the same as used by Langston et al. (1977) and Graziani et al. (1980), although, their tunnel used four blades with a rather low aspect ratio of approximately 1.0. Gostelow (1984) suggests an aspect ratio of 4.0 to achieve two-dimensional flow in a turbine cascade. The UCDavis cascade section had seven blades (nine blades including the end walls) with an aspect ratio of 3.56 while the USAFA cascade section had 5 blades (seven with end walls) with an aspect ratio of 3.97. Due to the favorable pressure gradient through the turbine cascade, boundary layer bleeds are not required (Gostelow, 1984). With an aspect ratio of 1.0, Graziani (1980) found the pressure surface to be essentially two-dimensional, but the suction surface was still dependent on the inlet boundary layer size.

In both test facilities the present study used a turbine airfoil shape with a very long history. It was first used in cascade tests by Langston et al. (1977). It is also geometrically similar to the mean blade geometry used in rotating tests by Dring et al. (1986) and Blair et al. (1989a, 1989b). The turbine blade shape is shown in

Figure 2. The physical coordinates of the turbine blade are listed in Butler (1995). The turbine blade shape is that of a heavily loaded machine with a design flow coefficient of .78, stage loading coefficient of 2.8, and 34% static pressure reaction [Blair et al. (1989a), (1989b)]. The turbine blade has an inlet mean camber line of 44° and an exit mean camber line is 26°. The air inlet angle was 44.7° at UCDavis (giving -0.7° of incidence) and 49° at USAFA. Locations on the turbine blade were measured relative to a geometric zero which is determined by placing a straight edge across the concave portion of the turbine blade. The tangent point near the leading edge is used as the reference point (s=0). Note, this location is not the stagnation point, although, this reference location is easier to duplicate and is consistent with Blair et al. (1989a, 1989b).

The turbine blades were hot-wire cut from dense polystyrene (2 lb/ft^3). Heat transfer tests were performed on the center blade in the cascade row.

For the heat transfer measurements, gold film was attached to the substrate (2 lb/ft^3 polystyrene) using 3-M spray adhesive (see Figure 2). The gold film is a thin 7-mil polyester sheet with vacuum deposited gold on the surface. The thin layer of gold provides the surface with a uniform electrical resistivity. Bus bars were formed using copper tape attached to each end of the gold film. To ensure good electrical contact a silver based paint was applied between the copper tape and the gold film.

The gold film was air brushed with flat black paint, followed by liquid crystals. The liquid crystals were narrow-band Hallcrest R40W1 (red beginning at 40° C and 1° bandwidth). Constant voltage is provided by a DC power supply to the copper bus bars. The voltage across the gold film causes current to flow through the gold film producing a nearly uniform Ohmic heating on the surface of the model. Since the polyester sheet and polystyrene blade act as an insulated surface, the uniform Ohmic heating produces a nearly uniform heat flux UHF convection from the surface. Current was measured using an Ammeter in series with the power supply. The voltage is measured using a voltmeter with separate lead wires to the bus bars (avoiding any voltage drop due to the resistance of the lead wires). The power can be determined by using the voltage and the current, current and resistance, or voltage and resistance. Because the resistance of the gold film changes slightly with temperature, the local value (at the temperature of the measured location) of the gold's resistance should be used. The clean tunnel free-stream turbulence was measured with a hot-wire to be approximately 0.5% and 1.0% in the USAFA and UCDavis cascade sections respectively.

A turbulence generating grid was used to simulate the high level of turbulence which exists in operating gas turbine engines. Grid turbulence theory and correlations provided in Baines and Peterson (1951), and Roach (1987) were used to design a square-mesh array of square bars. A 0.0381 m square-bar grid was placed 1.143 m upstream perpendicular to the flow at UCDavis. A 0.03175 m square-bar grid was placed 1.22 m upstream parallel to the cascade row at USAFA. Grid turbulence decays downstream of the grid and eddy scales increase. Assuming the turbulence to be isotropic and homogeneous, the turbulence length scales can be estimated using theory (Roach, 1987). For the UCDavis data, the grid turbulence macro-scale is estimated to be 0.0406 m and is independent of free-stream velocity. The micro-scale is estimated to be 0.0071 m (at 6 m/s) and 0.0051 m at 12 m/s.

DATA REDUCTION

The heat transfer measurements were begun by running the tunnel until it was at steady state. The electric power to the blade was then adjusted until a yellow color band (from the liquid crystals) appeared in a selected region of the model. The model was allowed to come to steady state while making minor adjustments to the power to keep the yellow color band in the region of interest. The low thermal conductivity of the blade model requires adequate time for this to occur..

Data reduction with the gold-film heated-coating (uniform heat flux or UHF) method is straight forward. The local heat transfer coefficient for the yellow lines is given by:

$$h = \frac{q_c''}{(T_{LC} - T_\infty)}$$

The adiabatic wall temperature can be used as the reference temperature (T_∞). In the present case, a thermocouple exposed to the free-stream tunnel air is used to measure temperature (T_∞). For this low Mach number flow, the measured temperature is within 0.1° C of the total, static, and adiabatic wall temperatures.

When steady state is reached, the lines of yellow color from the liquid crystals represent isothermal lines, which for a given heat flux (power setting) represent lines of constant heat transfer coefficient. Typical patterns for the color yellow at different power settings are shown in Figures 3a and 3b for the pressure and suction sides of the turbine blade respectively.

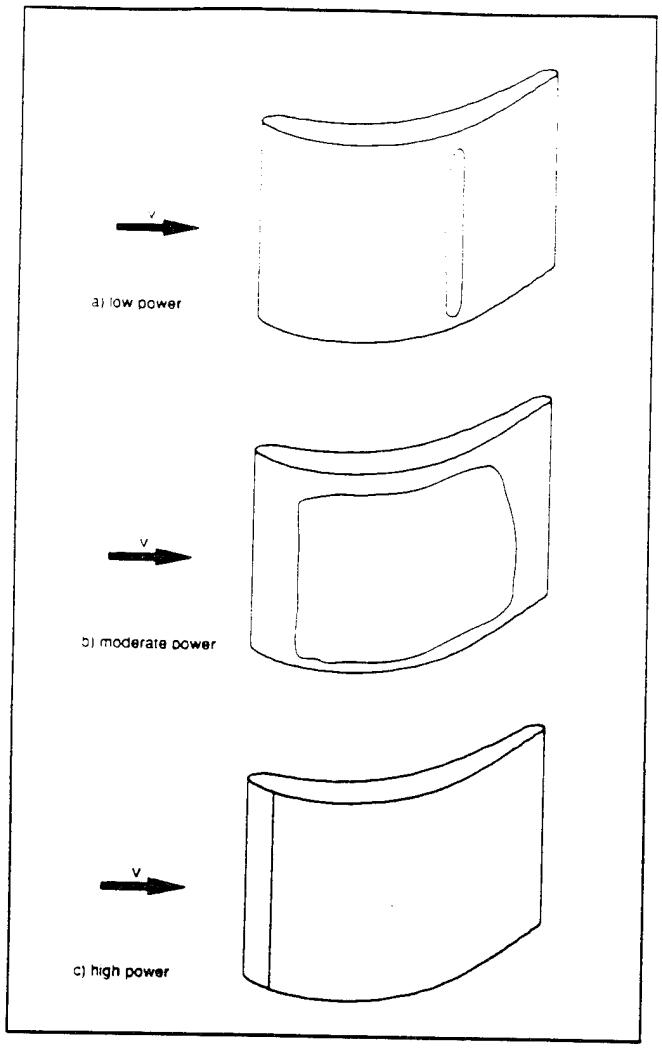

FIGURE 3A. SKETCH SHOWING THE YELLOW ISOTHERM ON THE SUCTION SURFACE

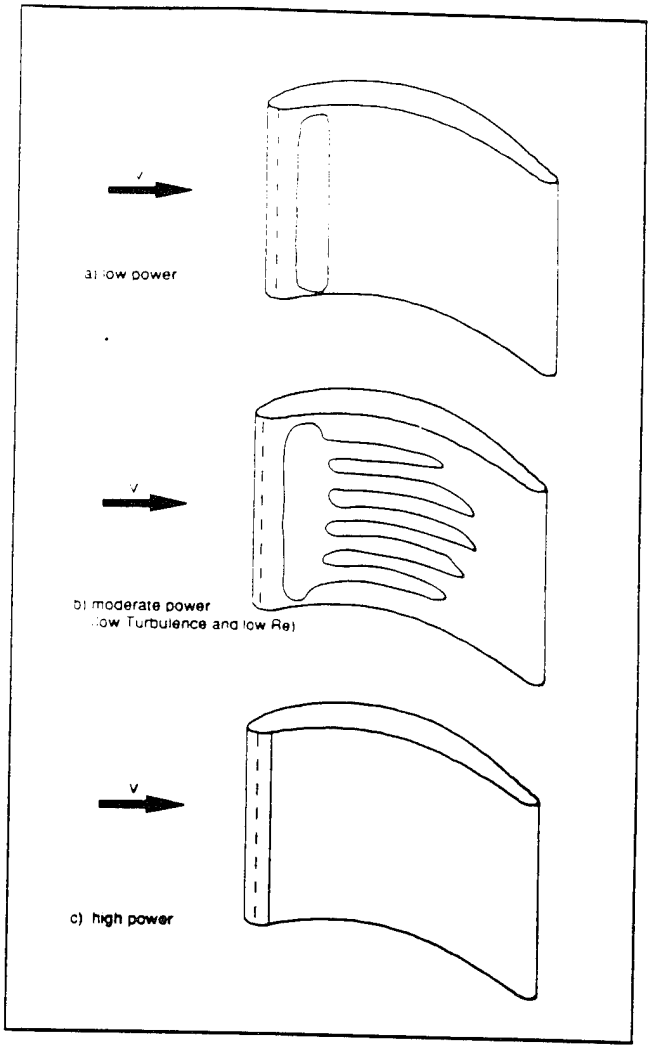

FIGURE 3B. SKETCH SHOWING THE YELLOW ISOTHERM ON THE PRESSURE SURFACE

The heat flux due to convection (q_c'') is determined by subtracting radiation and conduction losses from the local electrical heating per unit of surface area (q").

$$q_c'' = q'' - \varepsilon\sigma(T_{LC}^4 - T_\infty^4) - q_L''$$

The local electrical heating (q") is calculated using the following equation:

$$q'' = \frac{i^2 R_{40}}{hw} = \frac{i^2 (R_{40}'' l / w)}{hw} = \frac{i^2 R_{40}''}{w^2}$$

This equation accounts for the slight temperature sensitivity of the resistance of the gold coating. In the present method this is easy since the data is all collected at the same surface temperature (the yellow color of the liquid crystals). This equation uses the resistance of the gold coating at the yellow color (40° C) and assumes the current is uniform through the model. The current, length and width of the gold are measured. The resistance of the gold at 40° C (R_{40}) is expressed in terms of the resistance per square (R"). The resistance per square is a common way to express the resistance of surface coatings and it is simply the resistance of any size square piece (note: due to scaling of the electrical path, any size square piece will have the same resistance). The actual resistance of a rectangular piece is proportional to its length and inversely proportional to its width. The resistance of the gold sample was measured using a four-wire arrangement at 25° C to be 5.63 Ohms. Baughn et al. (1985) measured the temperature coefficient of the gold coating to be .0011 (1/C°). Therefore, the resistance of the coating would be R_{40}= 5.63(1+.0011(40-25)) = 5.72 Ohms at 40° C.

Accounting for the dimensions of the gold yields $R''_{40}=R_{40}(w/l)= 2.49$ Ohms/square.

The conduction losses (q_L'') are negligible for the turbine blade because the model is made from polystyrene. The radiation can not be ignored. The radiation component ranged from 3-21% in regions of very high or very low convective heat transfer.

The liquid crystal temperature (T_{LC}) was determined by using two different calibration techniques. The two methods gave consistent results showing the center of the yellow color band of the R40W1 liquid crystals to be 40.10° ±.15° C. More detail about the liquid crystal calibration is available in Butler (1995).

UNCERTAINTY ANALYSIS

An uncertainty analysis (using standard uncertainty methods and 95% confidence) was performed for the heat transfer measurements. The individual contributions to the uncertainty of the local heat transfer coefficient are given in Table II. The variation of the gold's local resistivity, estimated to be approximately 5%, is the largest contributor to the overall uncertainty. The total uncertainty is estimated to be approximately 6%. It is believed that this is conservative since the uniformity of the liquid crystal color during tests suggests the gold uniformity is probably better than the 5% estimate. The uncertainty in the Reynolds number is estimated to be 2%.

TABLE II. UNCERTAINTY ANALYSIS

Measured Parameter	Typical Value	δX (±)	h Uncertainty %
R"	2.49 Ohms/Sq	.125	5.0
T_∞	26.3° C	.15	1.2
T_{LC}	40.1° C	.15	1.2
L	18.375 in	.008	0
W	8.00 in	.008	.2
ε	85	.15	1.7
i	3.77 A	.005	.3
V	21.56 V	.005	0
			Total=5.5%

RESULTS

Aerodynamic Measurements

Free-stream turbulence intensity was measured using a constant temperature hot-film anemometer (details are also given in Butler, 1995). Without the grid in place, the turbulence level is independent of velocity and is nominally 1% at UCDavis and .5% at USAFA. With the grid, there was a natural decay of the turbulence as it traveled downstream. In this case, the turbulence intensity at the leading edge of the test blade was found by extrapolation from 1 inch upstream of the test blade giving a turbulence intensity of nominally 10% (grid design theory correctly predicted this result).

Wake velocity measurements were also taken in the UCDavis tests using the TSI constant temperature hot-film anemometer. The wake velocities are given in Butler (1995). The favorable pressure gradient across the cascade produced a velocity increase through the cascade. Based on the hot-film measurements and a spatial average of the wake velocities, on average the exit velocity is 65% larger than the free-stream velocity. Many researchers use cascade exit conditions to normalize their results. The present work uses inlet conditions, although the present Reynolds and Stanton numbers could be based on exit conditions by increasing the velocity by 65%.

Heat Transfer Measurements

The heat transfer data taken in the UCDavis linear cascade will be presented and discussed first (comparisons of the UCDavis and USAFA measurements are made later). The results for the low Reynolds number used (67,500) are shown in Figure 4 for the two different turbulence intensities and for higher Reynolds numbers (134,000 and 144,000) in Figure 5. Discussions of the distributions on the leading edge, the suction side and the pressure side follow in order. The effect of the Reynolds number is then discussed.

The heat transfer results (Stanton number) were based on inlet flow conditions. Except where noted, the heat transfer results were spanwise uniform due to the high aspect ratio of the blades.

In the region of the leading edge, which is cylindrical in shape, the heat transfer behaves very much like the forward region of a cylinder in cross-flow. The highest heat transfer exists at the stagnation point of the leading edge (which corresponds to s/Bx=.03). As seen in

Figure 4, as the boundary layer grows the local heat transfer decreases rapidly in the region from s/Bx=.03 to .15 (on the suction surface) and s/Bx=.03 to -.11 (on the pressure surface). In this leading edge region, the shape of the distribution is not changed by the turbulence intensity, but the higher turbulence intensity (10%) has a higher heat transfer level. In fact, the grid turbulence increases the heat transfer by 13% at the stagnation point for the Reynolds number of 67,500. This is consistent with Lowery and Vachon (1975), and the many others who have investigated turbulence effects on the stagnation region of a cylinder.

On the suction surface, the flow continues to accelerate from s/Bx=.15 to roughly s/Bx=0.6 and the heat transfer decreases much like laminar flow over a plate for both 1% and 10% turbulence intensities. The shapes of the curves are the same for both turbulence intensities with a higher heat transfer for the higher turbulence intensity (roughly 12% above that for the low intensity case). The favorable pressure gradient in this region clearly helps the boundary layer stay laminar. The flow goes through an adverse pressure gradient (as it decelerates) from roughly s/Bx=0.6 to the end of the suction surface. This can cause the boundary layer to transition or can cause flow separation. Boundary layer transition would cause the heat transfer to increase in the transition region, followed by decreasing levels as the fully turbulent boundary layer grows. If the boundary layer separates, the heat transfer would be low in the separated region. Looking again at Figure 4 (low Reynolds number), it can be seen that on the suction side, with s/Bx greater than 1.0, the heat transfer continues to decrease for the low turbulence intensity (1%) case, but increases for the high turbulence intensity (10%) case. For the low intensity case, there appears to be two minimums, both with very low heat transfer levels. Because of the low Reynolds number and turbulence level, it was suspected that one of these minimums was boundary layer separation. This was confirmed by laser tuft measurements described below. For the high intensity case, the heat transfer increases, a clear sign of boundary layer transition. Looking at Figure 5, it can be seen that the low heat transfer and second minimum for s/Bx greater than 1.0 do not occur.

On the pressure surface with low turbulence (see Figure 4 again), the flow decelerates slightly over a short region (from s/Bx=-.11 to -.22), the laminar boundary layer grows and the heat transfer decreases. From s/Bx=-.22 to the end of the pressure surface, the flow encounters strong concave curvature. In this region, the appearance of the liquid crystal colors is different for the low turbulence intensity versus high turbulence intensity cases. The concave surface seems to hold the heat transfer relatively constant at turbulent levels. When the boundary layer is still laminar, the concave curvature region has spanwise variation in the heat transfer which could be caused by Taylor-Görtler (discussed in the next section) vortices which form and enhance the heat transfer, but the overall level is still below that of a turbulent boundary layer.

Now consider the pressure side heat transfer distributions (also shown in Figure 4). For both levels of turbulence intensity, the curves show decreasing heat transfer as the laminar boundary layer grows from the stagnation point to s/Bx=-.16 (although, the higher turbulence case has higher heat transfer by an average of 23% in this region). At s/Bx=-.16, the heat transfer for the low turbulence case continues to decrease until s/Bx=-.22 thereafter increasing slowly while the heat transfer for high turbulence increases rapidly and then levels off. Not only is there a difference in the average level of heat transfer but there is a totally different appearance in the liquid crystal color distributions for these two different turbulence levels. For the low turbulence levels there was spanwise variation of the local heat transfer coefficient which was evident by liquid crystal "color fingers". This is shown in Figure 3b.

The effect of these spanwise variations on the heat transfer are shown in Figure 4 by showing both the maximum and minimum heat transfer for any span location. These "fingers" could possibly be Taylor-Görtler vortices which form on the concave portion of the pressure surface with a laminar boundary layer. If this were the case, the high heat transfer regions are produced by downflow between vortices and the low heat transfer regions are formed by upflow. Taylor-Görtler vortices have been found on concave surfaces by many investigators. Mayle et al. (1979) measured spanwise variation of dynamic pressure, Han and Cox (1983) took high speed smoke photographs, and Priddy and Bayley (1988) used a laser-Doppler anemometer to show the presence of Taylor-Görtler vortices on a turbine blade. Crane and Sabzvari (1989) used a uniform heat flux liquid crystal technique to measure the heat transfer and visualize the Taylor-Görtler vortices on the concave section of a water tunnel. While it is uncertain in the present case whether Taylor-Görtler vortices account for these "fingers" the high sensitivity of this experimental technique allows small variations to be seen.

The high turbulence intensity data does not have these "fingers" and has relatively level high heat transfer rates. Overall on the concave portion of the pressure surface, the high turbulence intensity case produces nearly double the heat transfer rate of the low turbulence case.

The effect of Reynolds number can be seen by comparing Figure 4 (Reynolds number of 67,000) to Figure 5 (Reynolds number of 134,000 and 144,000).

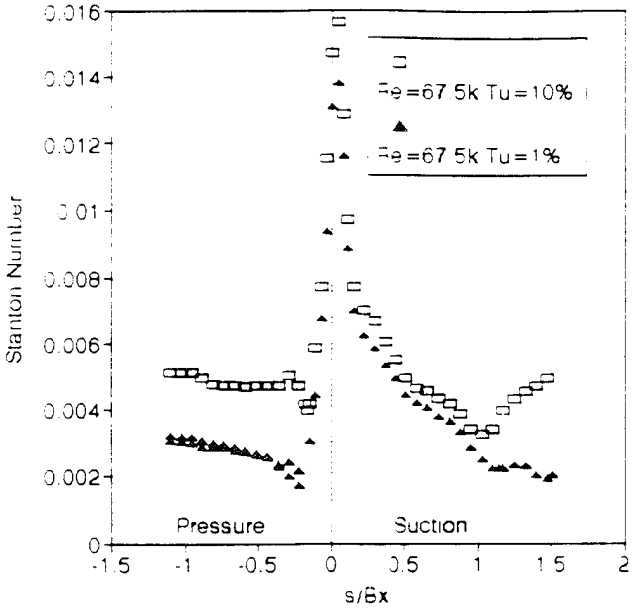

FIGURE 4. EFFECT OF TURBULENCE AT LOW REYNOLDS NUMBER (UCDAVIS)

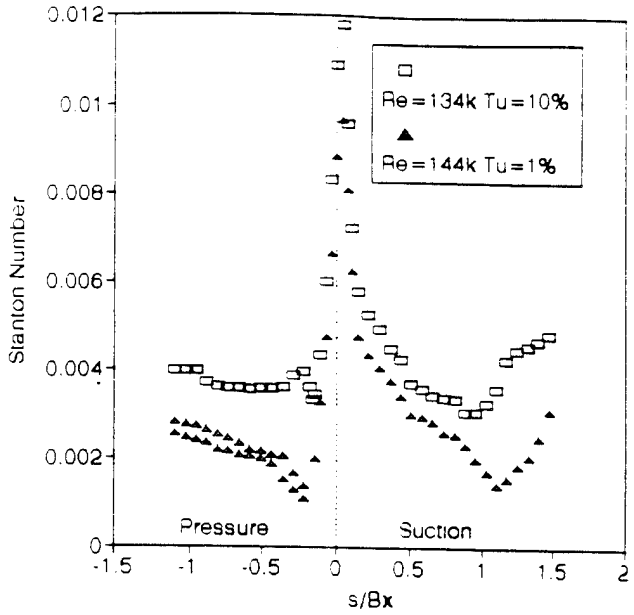

FIGURE 5. EFFECT OF TURBULENCE AT HIGHER REYNOLDS NUMBER (UCDAVIS)

A comparison of the data at the different Reynolds number of Figures 4 and 5 can be misleading since the Stanton number is inversely proportional to velocity, while laminar heat transfer is proportional to the square-root of velocity and turbulent heat transfer is proportional to velocity to the 0.8 power. Therefore for the present study, when the Reynolds number is not exactly matched, the quoted differences in laminar heat transfer are adjusted for the square-root of velocity (the plotted values are not adjusted).

In the leading edge region at the higher Reynolds number of Figure 5 (134,000) the turbulence increases the stagnation point heat transfer by 17% (compared to 13% at Re=67,500). For a fixed increase in turbulence, Lowery and Vachon (1975) also found higher percentage changes to the stagnation heating for larger Reynolds numbers.

On the suction surface with higher Reynolds number, the heat transfer is elevated in the laminar boundary layer growth region by an average of roughly 16%. The laminar boundary layer region percentage increase is slightly less than the increase at stagnation, which was also the case at the lower Reynolds number. This would agree with Kestin (1966), and Junkhan and Serovy (1967) who showed that turbulence increases the heat transfer for laminar boundary layers with favorable pressure gradients. For these higher Reynolds numbers, both turbulence levels show boundary layer transition (no separation such as occurred at lower Reynolds number). The higher grid turbulence advances the transition location to s/Bx=.92, as compared to s/Bx=1.1 for the low turbulence condition. Dullenkopf and Mayle (1994) also showed that added turbulence advances the boundary layer transition location on the suction surface. On the pressure surface, the results at a higher Reynolds number are similar to those for the lower Reynolds number. The laminar boundary layer grows with decreasing heat transfer from the stagnation point, until the spanwise variation again forms for the low turbulence intensity case. As before, at high turbulence intensity these spanwise variations disappear and the the heat transfer levels nearly double.

Laser-Tuft Results

For the low intensity measurements on the suction side of a blade, it was desired to confirm that flow separation had occurred. For example, in Figure 4 at s/Bx greater than 1.0 there are two small heat transfer minimums. In order to determine if one of these was flow separation, a technique suggested by Baughn and Rivir (1994) was used to non-intrusively determine the flow direction on the blade surface. A 20 mW Helium-Neon laser was used in conjunction with the liquid-crystal coated gold-film heater. Power was applied to the gold film to bring this location very near, but below ,the liquid crystal color play temperature. The location of interest was then further heated using the laser. The laser heated a small (~3 mm)

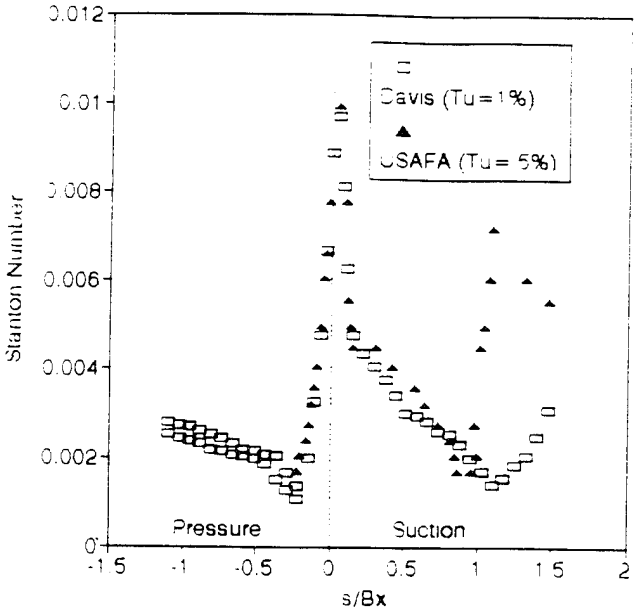

FIGURE 6. UCDAVIS (Re=144K) AND USAFA (Re=110K) RESULTS AT LOW TURBULENCE

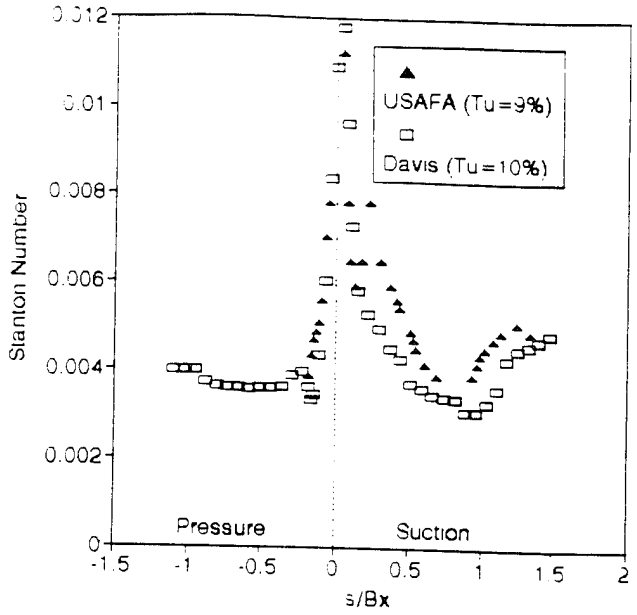

FIGURE 7. UCDAVIS (Re=134K) AND USAFA (Re=110K) RESULTS AT HIGHER TURBULENCE

circle to a temperature above the liquid crystal color play temperature. The laser was then turned off and the color shape was observed. The laser produced a hot spot which advected in the direction of the surface flow and this flow direction was detected by a "tail" of color from the circle. This can be referred to as a "liquid crystal thermal tuft" or simply "LC thermal tuft". The LC thermal tuft showed that the flow continued down the blade at the first minimum, but didn't seem to have any direction at the second minimum. This would suggest that the second minimum is boundary layer separation. In future measurements, it is planned to use either a beam splitter or multiple measurements and obtain a matrix of tufts. In this case, we refer to this as a Laser Tuft Matrix (LTM) method. It is also possible to do this with other surface optical temperature sensors, such as phosphors.

Comparison of UCDavis and USAF Academy Results

Two sets of data were collected in the USAFA linear cascade. Data was collected with and without a turbulence grid at a Reynolds number of 110,000. These results are compared with the UCDavis high Reynolds number data in Figures 6 and 7 for the low and high turbulence levels respectively. For the USAFA data, the grid turbulence again had a major effect on the magnitude and the general profile of the heat transfer distributions.

In the leading edge region the results for the USAFA and UCDavis data are similar with an increase of 13% in the stagnation point heat transfer for 9% grid turbulence in the USAFA data. These results are at slightly different free-stream velocities (12 m/s at UCDavis and 12.5 m/s at USAFA), therefore due to the inverse relation of Stanton number to velocity, the results do not match at the stagnation point.

On the suction surface with low turbulence levels (Figure 6) the heat transfer distribution measured at USAFA is dramatically different from that measured at UCDavis. At USAFA the heat transfer decreases as a laminar boundary layer grows from the stagnation point up to s/B_x=.921 (similar to what occurred in the UCDavis data). At this point, the laminar boundary layer appears to separate, followed by very high heat transfer where the boundary layer reattaches at s/B_x= 1.09 (whereas the UCDavis data shows transition but does not show separation). The difference is attributed to the larger blade spacing and pitch/axial chord of the USAFA cascade. As the turbine blades are moved farther apart, the flow separates because it is unable to navigate the large turning angle. This has been confirmed in current research specifically investigating the effect of blade spacing.

On the suction surface with high turbulence levels, the USAFA distribution is slightly different from the UCDavis data. It shows a minimum at s/B_x=.132 and a maximum at s/B_x=.226. This profile could be caused by a flow

condition with overspeed (where the heat transfer increase is due to rapid acceleration) or by flow with weak separation followed by laminar reattachment. Either flow condition could be caused by an increased flow incidence angle due the the placement of the square-bar grid at an angle to the free-stream velocity (parallel to the cascade plane). After s/B_x=.226 with the grid, the heat transfer behaves like a growing laminar boundary layer. With higher turbulence in the USAFA tunnel, the laminar boundary layer does not separate at s/B_x=.921, instead it transitions to turbulent with a gradual rise in heat transfer followed by a decrease when the boundary becomes fully turbulent.

Comparison of Cascade and Rotating Data

The question of using a linear cascade to model the complex process of a rotating machine can always be debated. Guenette et al. (1989) concluded that rotating midspan data is largely two-dimensional and that cascade data (Ashworth et al., 1985) is qualitatively the same, though 50% differences existed in some regions. Therefore, in the present investigation, it was important to have a test case to compare with the cascade data. As mentioned earlier, a complete set of rotating tests for the same blade geometry was performed by Blair's group over the last decade. Most of their results are for Reynolds numbers higher than the present investigation, although, they did perform one set of tests which was not included in Blair et al. (1989b), but was tabulated in Dring et al. (1986). The present investigation matched their condition by running Re=134,000 and 10% turbulence.

Blair et al. (1989b) used a 1 1/2 stage (stator, rotor, stator) rotating rig. They looked at Reynolds number and turbulence effects. They found that adding a grid didn't effect their rotor results very much because the stator wakes produce turbulence which interact with the rotor. The test specifications for the present cascade are compared to Dring et al. (1986) in Table III.

A comparison of Dring's (1986) rotating test to the present results are shown in Figure 8. Both tests used a 10% grid. The results are nearly identical near the stagnation region and on the pressure surface. Previous comparisons [Blair et al. (1989b) versus Graziani et al. 1980)] on the pressure surface showed the cascade data being too low. On the suction surface the results are the same up to boundary layer transition. The transition location for the rotating test is further forward (s/Bx=.473) than the cascade test (s/Bx=.92). This was also true at higher Reynolds number in Blair's (1989b)comparison with cascade data by Graziani et al. (1980). This difference could have many sources, some possibilities

TABLE III. UCDAVIS CASCADE AND UTRC TEST SPECIFICATIONS

	Present Cascade	UTRC Rotating Rig
Axial Chord (B_x)	0.171 m	0.161 m
Pitch/Axial Chord (p/B_x)	.93	.96
Aspect Ratio	3.57	.95
Inlet Camber Angle	44°	42°
Exit Camber Angle	26°	26°
Air Inlet Angle	44.7°	40°
Exit Velocity	19.8 m/s	19.6 m/s

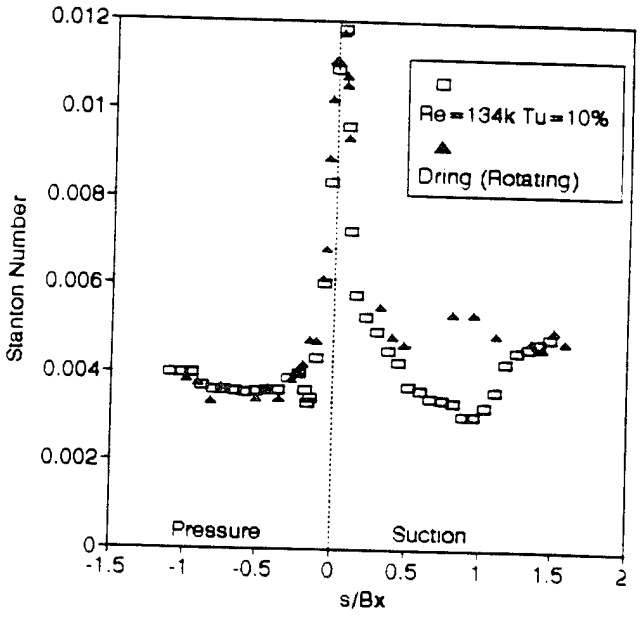

FIGURE 8. A COMPARISON OF LINEAR CASCADE (UCDAVIS) AND ROTATING (UTRC) RESULTS

would be: stator wake turbulence, three dimensional effects, surface roughness, or slight solidity differences. The max-to-min surface roughness for Dring's (1986) rotating data is 51 microns (Blair, 1994), while the present model surface roughness is estimated to be 10 microns. At low Reynolds number, Blair (1994) showed that increasing the surface roughness can advance the suction side transition location.

CONCLUSIONS

The present study investigated the effect of turbulence intensity and Reynolds number on turbine blade local heat transfer. The results show many interesting features of the turbine blade heat transfer distribution.

Turbulence intensity has a large effect on the local heat transfer. Increasing the turbulence intensity from 1% to 10% had the following three major effects on heat transfer: 1.) the heat transfer level increases, 2.) the suction side boundary layer transition location moves upstream, and 3.) the spanwise variation on the pressure side disappears.

At the stagnation point the heat transfer increased 13% at Re=67,500 and 17% at Re=134,000. The suction side laminar boundary layer heat transfer increased by an average of 12% at Re=67,500 and 16% at Re=134,000.

The grid turbulence causes the suction side boundary layer transition location to move upstream from s/Bx=1.1 to s/Bx=.92 for the Reynolds number of 134,000.

In the concave curvature region of the pressure surface the turbulence level has a significant effect. With 1% turbulence, the heat transfer varied spanwise in a somewhat periodic distribution. One possible explanation for this is the presence of Taylor-Görtler vortices in the laminar boundary layer. With 10% turbulence the spanwise variation did not occur, but the heat transfer nearly doubled. If the spanwise variation is caused by the presence of Taylor Görtler vortices, they did not occur with the higher turbulence level.

The effect of Reynolds number on the results were different with and without the grid. Without the grid, the suction side boundary layer separated at Re=67,500 and it transitioned to turbulent at Re=134,000. With the grid, the suction side boundary layer transition point moved forward (from s/Bx=1.03 to .92) when the Reynolds number increased (from Re=67,500 to 134,000). The results showed that the effect of turbulence is dependent on the Reynolds number. For example, for a given percentage increase in turbulence intensity, there was a larger percentage increase in heat transfer when the Reynolds number is increased. This has been observed by others for the stagnation region of a cylinder.

The results were also compared to tests performed in the USAF Academy Cascade tunnel. At low turbulence levels, the USAFA data showed boundary layer separation on the rear portion of the suction side. Subsequent investigations show that this was caused by the larger blade spacing in the USAFA cascade. With grid turbulence, the USAFA results had a maximum and minimum near the front of the suction surface. It is believed that this is caused by the change in flow incidence in the USAFA cascade. This was produced by the square bar grid which was installed in the USAFA cascade tunnel parallel to the cascade plane (at an angle relative the free-stream flow).

One continuing concern with cascade data has been that it lacks rotational effects. It is reassuring that the present cascade data compares very favorably to rotational data collected by Dring et al. (1986). The present heat transfer results are nearly the same in the stagnation, laminar suction surface, and the pressure surface regions as those of Dring et al. (1986). The boundary layer transition location on the suction surface was advanced in the rotating tests.

REFERENCES

Ainsworth, R. W., Allen, J. L., Davies, M. R. D., Doorly, J. E., Forth, C. J. P., Hilditch, M. A., Oldfield, M. L. G., and Sheard, A. G. 1989, "Developments in Instrumentation and Processing for Transient Heat Transfer Measurement in a Full-Stage Model Turbine," ASME *Journal of Turbomachinery*, Vol. 111, pp. 20-27.

Ashworth, D. A., LaGraff, J. E., Scultz, D. L., and Grindrod, K. J. 1985, "Unsteady Aerodynamic and Heat Transfer Processes in a Transonic Turbine Stage," *Journal of Engineering for Gas Turbines and Power*, Vol. 107, pp. 1022-1030.

Baines, W. D., and Peterson, E. G., 1951, "An Investigation of Flow Though Screens", *Transactions of ASME*, Vol 73, pp. 467-480.

Baughn, J. W., Takahashi, R. K., Hoffman, M. A., and McKillop, A. A. 1985, "Local Heat Transfer Measurements using an Electrically Heated Thin Gold-Coated Plastic Sheet," ASME *Journal of Heat Transfer*, Vol. 107, pp 953-959.

Baughn, J. W., Ireland, P. T., Jones, T. V., and Saniei, N. 1989, "A Comparison of the Transient and Heated-Coating Methods for the Measurements of the Local Heat Transfer Coefficients on a Pin Fin," ASME *Journal of Heat Transfer*, Vol. 111, pp 877-881.

Baughn, J. W. and Rivir, R. B., personal communication, 1994.

Blair, M. F., Dring, R. P., and Joslyn, H. D. 1989a, "The Effects of Turbulence and Stator/Rotor Interactions on Turbine Heat Transfer: Part 1-Design Operating Conditions," ASME *Journal of Turbomachinery*, Vol. 111, pp. 87-96.

Blair, M. F., Dring, R. P., and Joslyn, H. D. 1989b, "The Effects of Turbulence and Stator/Rotor Interactions on Turbine Heat Transfer: Part 2-Effects of Reynolds Number and Incidence," ASME *Journal of Turbomachinery*, Vol. 111, pp. 97-103.

Blair, M. F. 1994, "An Experimental Study of Heat Transfer in a Large-Scale Turbine Rotor Passage," ASME *Journal of Turbomachinery*, Vol. 116, pp. 1-13.

Boyle, R. J., and Russell, L. M. 1990, "Experimental Determination of Stator Endwall Heat Transfer," *Journal of Turbomachinery*, Vol. 112, pp. 547-557.

Boyle, R. J. 1991, "Navier-Stokes Analysis of Turbine Blade Heat Transfer," *Journal of Turbomachinery*, Vol. 113, pp. 392-403.

Butler, R. J. 1995, "The Effects of the Thermal Boundary Condition and Turbulence on Heat Transfer from a Cylinder, Flat Plate, and Turbine Blade using the Transient Shroud and Heated-Coating Techniques," PhD Dissertation, University of California Davis.

Cooper, T. E., Field, R. J., and Meyer, J. F., 1975, "Liquid Crystal Thermography and its Application to the Study of Convective Heat Transfer," *Journal of Heat Transfer*, pp. 442-450.

Crane, R. I., and Sabzvari, J. 1989, "Heat Transfer Visualization and Measurement in Unstable Concave-Wall Laminar Boundary Layers," ASME *Journal of Turbomachinery*, Vol. 111, pp. 51-56.

Dring, R. P., Blair, M. F., and Joslyn, H. D., 1986, "The Effects of Inlet Turbulence and Rotor Stator Interactions on the Aerodynamic and Heat Transfer of a Large-Scale Rotating Turbine Model, Vol II- Heat Transfer Data Tabulation, 15% Axial Spacing," NASA CR 179467, UTRC-R86-956480-2.

Dullenkopf, K., Schulz, A., and Wittig, S. 1991, "The Effect of Incident Wake Conditions on the Mean Heat Transfer of an Airfoil," *Journal of Turbomachinery*, Vol. 113, pp. 412-418.

Dullenkopf, K., and Mayle, R. E. 1994, "The Effects of Incident Turbulence and Moving Wakes on the Laminar Heat Transfer in Gas Turbines," ASME *Journal of Turbomachinery*, Vol. 116, pp. 23-28.

Dunn, M. G., and Stoddard, F. J., 1979, "Measurement of Heat Transfer Rate to a Gas Turbine Stator," *Journal of Engineering for Power*, Vol. 101, pp. 275-280.

Dunn, M. G., Rae, W. J., and Holt, J. L. 1984a, "Measurement and Analyses of Heat Flux Data in a Turbine Stage: Part 1-Description of Experimenatal Apparatus and Data Analysis," *Journal of Engineering for Gas Turbines and Power*, Vol. 106, pp. 229-233.

Dunn, M. G., Rae, W. J., and Holt, J. L. 1984b, "Measurement and Analyses of Heat Flux Data in a Turbine Stage: Part 2-Discussion of Results and Comparison with Predictions," *Journal of Engineering for Gas Turbines and Power*, Vol. 106, pp. 234-240.

Dunn, M. G., and Chupp, R. E. 1988, "Time-Averaged Heat-Flux Distributions and Comparison with Prediction for the Teledyne 702 HP Turbine Stage," *Journal of Turbomachinery*, Vol. 110, pp. 51-56.

Dunn, M. G., Seymour, P. J., Woodward, S. H., George, W. K., and Chupp, R. E. 1989, "Phase-Resolved Heat-Flux Measurements on the Blade of a Full-Scale Rotating Turbine," *Journal of Turbomachinery*, Vol. 111, pp. 8-19.

Dunn, M. G. 1990, "Phase and Time-Resolved Measurements of Unsteady Heat Transfer and Pressure in a Full-Stage Rotating Turbine," *Journal of Turbomachinery*, Vol. 112, pp. 531-538.

Dunn, M. G., Kim, J., Civinskas, K. C., and Boyle, R. J. 1994, "Time-Averaged Heat Transfer and Pressure Measurements and Comparison with Prediction for a Two-Stage Turbine," *Journal of Turbomachinery*, Vol. 116, pp. 14-22.

Gostelow, J. P., 1984, *Cascade Aerodynamics*, Pergamon Press, Oxford, England.

Giedt, W. H. 1949, "Investigation of Variation of Point Unit Heat Transfer Coefficient Around a Cylinder Normal to an Air Stream," *Transactions of the ASME*, Vol. 71, pp. 375-381.

Graziani, R. A., Blair, M. F., Taylor, J. R., and Mayle, R. E. 1980, "An Experimental Study of Endwall and Airfoil Surface Heat Transfer in a Large Scale Turbine Blade Cascade," *Journal of Engineering for Power*, Vol. 102, pp. 257-267.

Guenette, G. R., Epstein, A. H., Giles, M. B., Haimes, R. and Norton, R. J. G. 1989, "Fully Scaled Transonic Turbine Rotor Heat Transfer Measurements," *Journal of Turbomachinery*, Vol. 111, pp. 1-7.

Han, L. S., and Cox, W. R. 1983, "A Visual Study of Turbine Blade Pressure-Side Boundary Layers," *Journal of Engineering for Power*, Vol. 105, pp. 47-52.

Hippensteele, S. A., Russell, L. M., and Torres, F. J. 1985, "Local Heat-Transfer Measurements on a Large Scale-Model Turbine Blade Airfoil using a Composite of a Heater Element and Liquid Crystals," *Journal of Engineering for Gas and Power*, Vol. 107, pp. 953-960.

Harasgama, S. P., and Wedlake, E. T. 1991, "Heat Transfer and Aerodynamics of a High Rim Speed Turbine Nozzle Guide Vane Tested in the RAE Isentropic Light Piston Cascade (ILPC)," *Journal of Turbomachinery*, Vol. 113, pp. 384-391.

Junkhan, G. H., and Serovy, G. K. 1967, "Effects of Free-Stream Turbulence and Pressure Gradient on Flat-Plate Boundary-Layer Velocity Profiles and on Heat Transfer," *Journal of Heat Transfer*, pp. 169-176.

Kestin, J. 1966, "The Effect of Free-Stream Turbulence on Heat Transfer Rates," *Advances in Heat Transfer*, Vol. 3, pp. 1-31.

Langston, L. S., Nice, M. L., and Hooper, R. M. 1977, "Three-Dimensional Flow within a Turbine Cascade Passage," *Journal of Engineering for Power*, Vol. 99, pp. 21-28.

Lakshminarayana, B., Camci, C., Halliwell, I., and Zaccaria, M., 1992, "Investigation of Three Dimensional Flow Field in a Turbine including Rotor/Stator Interaction, Part1: Design Development and Performance of the Research Facility," American Institute of Aeronautics and Astronautics.

Lowery, G. W., and Vachon, R. I. 1975, "The Effect of Turbulence on Heat Transfer from Heated Cylinders," *Int. Journal of Heat and Mass Transfer*, Vol. 18, pp. 1229-1242.

Mayle, R. E., Blair, M. F., and Kopper, F. C. 1979, "Turbulent Boundary Layer Heat Transfer on Curved Surfaces," ASME *Journal of Heat Transfer*, Vol. 101, pp 521-525.

Moore, J., and Ransmayr, A. 1984a, "Flow in a Turbine Cascade: Part 1- Losses and Leading-Edge Effects," *Journal of Engineering for Gas Turbines and Power*, Vol. 106, pp. 401-408.

Moore, J., and Ransmayr, A. 1984b, "Flow in a Turbine Cascade: Part 2- Measurement of Flow Trajectories by Ethylene Detection," *Journal of Engineering for Gas Turbines and Power*, Vol. 106, pp. 409-413.

Moore, J., and Adhye, R. Y. 1985, "Secondary Flows and Losses Downstream of a Turbine Cascade," *Journal of Engineering for Gas Turbines and Power*, Vol. 107, pp. 961-968.

Moore, J., and Moore, J. G. 1985, "Performance Evaluation of Linear Turbine Cascades Using Three-Dimensional Viscous Flow Calculations," *Journal of Engineering for Gas Turbines and Power*, Vol. 107, pp. 969-975.

Moore, J., Shaffer, D. M., and Moore, J. G. 1987, "Reynolds Stresses and Dissipation Mechanisms Downstream of a Turbine Cascade," *Journal of Turbomachinery*, Vol. 109, pp. 258-267.

Nealy, D. A., Mihelc, M. S., Hylton, L. D., and Gladden, H. J. 1984, "Measurements of Heat Transfer Distribution over the Surfaces of Highly Loaded Turbine Guide Vanes," *Journal of Engineering for Gas Turbines and Power*, Vol. 106, pp. 149-158.

O'Brien, J. E., Simoneau, R. J., LaGraff, J. E., and Morehouse, K. A. 1986, "Unsteady Heat Transfer and Direct Comparison for Steady-State Measurements in a Rotor-Wake Experiment", *Proceedings, 8th International Heat Transfer Conference*, San Francisco, pp. 1243-1248.

Priddy, W. J., and Bayley, F. J. 1988, "Turbulence Measurements in Turbine Blade Passages and Implications for Heat Transfer," *Journal of Turbomachinery*, Vol. 110, pp. 73-79.

Roach, P. E., 1987, "The Generation of Nearly Isotropic Turbulence by Means of Grids," *Heat and Fluid Flow*, Vol. 8, No 2, pp 82-92.

Schultz, D. L., and Jones, T. V. 1973, "Heat Transfer Measurements in Short Duration Hypersonic Facilities," Agardograph No. 165.

Schultz, D. L., Oldfield, M. L. G., and Jones, T. V. 1980, "Heat Transfer Rate and Film Cooling Effectiveness Measurements in a Transient Cascade," AGARD CP-281.

Simoneau, R. J., and Simon, F. F. 1993, "Progress Torwards Understanding and Predicting Heat Transfer in the Turbine Gas Path," *International Journal of Heat and Fluid Flow*, Vol. 14, No. 2, pp. 106-128.

Simonich, J. C., and Bradshaw, P. 1978, "Effect of Free-Stream Turbulence on Heat Transfer through a Turbulent Boundary Layer," ASME *Journal of Heat Transfer*, Vol. 100, pp 671-677.

Turner, A. B. 1971, "Local Heat Transfer Measurements on a Gas Turbine Blade," *Journal Mechanical Engineering Science*, Vol. 13, pp. 1-12.

Wedlake, E. T., Brooks, A. J., and Harasgama, S. P. 1989, "Aerodynamic and Heat Transfer Measurements on a Transonic Nozzle Guid Vane," *Journal of Turbomachinery*, Vol. 111, pp. 36-42.

Wilson, D. G., and Pope, J. A. 1954, "Convective Heat Transfer to Gas Turbine Blade Surfaces," *Proceedings Institutional Mechanical Engineering*, Vol. 168, pp. 861-874.

York, R. E., Hylton, L. D., and Mihelc, M. S. 1984, "An Experimental Investigation of Endwall Heat Transfer and Aerodynamics in a Linear Vane Cascade," *Journal of Engineering for Gas Turbines and Power*, Vol. 106, pp. 159-167.